

# Initiator Control of Conjugated Polymer Topology in Ring-Opening Alkyne Metathesis Polymerization

Stephen von Kugelgen,<sup>†,‡,§</sup> Donatela E. Bellone,<sup>†,‡</sup> Ryan R. Cloke,<sup>†</sup> Wade S. Perkins,<sup>†</sup> and Felix R. Fischer<sup>\*,†,‡,§</sup>

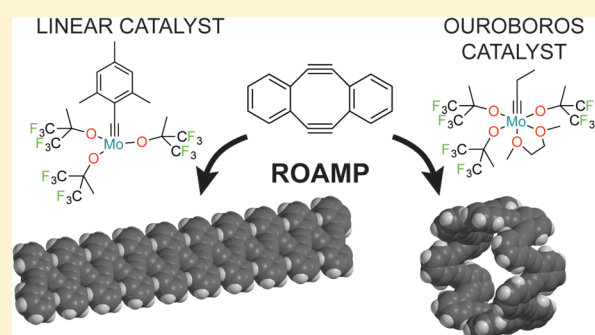
<sup>†</sup>Department of Chemistry, University of California, Berkeley, California 94720, United States

<sup>‡</sup>Materials Sciences Division, Lawrence Berkeley National Laboratory, Berkeley, California 94720, United States

<sup>§</sup>Kavli Energy Nanosciences Institute at the University of California Berkeley and Lawrence Berkeley National Laboratory, Berkeley, California 94720, United States

## S Supporting Information

**ABSTRACT:** Molybdenum carbyne complexes  $[\text{RC}\equiv\text{Mo}(\text{OC}(\text{CH}_3)(\text{CF}_3)_2)_3]$  featuring a mesityl ( $\text{R} = \text{Mes}$ ) or an ethyl ( $\text{R} = \text{Et}$ ) substituent initiate the living ring-opening alkyne metathesis polymerization of the strained cyclic alkyne, 5,6,11,12-tetrahydrobenzo[*a,e*][8]annulene, to yield fully conjugated poly(*o*-phenylene ethynylene). The difference in the steric demand of the polymer end-group ( $\text{Mes}$  vs  $\text{Et}$ ) transferred during the initiation step determines the topology of the resulting polymer chain. While  $[\text{MesC}\equiv\text{Mo}(\text{OC}(\text{CH}_3)(\text{CF}_3)_2)_3]$  exclusively yields linear poly(*o*-phenylene ethynylene), polymerization initiated by  $[\text{EtC}\equiv\text{Mo}(\text{OC}(\text{CH}_3)(\text{CF}_3)_2)_3]$  results in cyclic polymers ranging in size from  $n = 5$  to 20 monomer units. Kinetic studies reveal that the propagating species emerging from  $[\text{EtC}\equiv\text{Mo}(\text{OC}(\text{CH}_3)(\text{CF}_3)_2)_3]$  undergoes a highly selective intramolecular backbiting into the butynyl end-group.



undergoes a highly selective intramolecular backbiting into the butynyl end-group.

## INTRODUCTION

Semiconducting  $\pi$ -conjugated polymers have been widely explored as functional materials in advanced electronic devices. They combine the superior processability and mechanical performance of polymers with readily tunable optical, electrical, and magnetic properties of small molecules.<sup>1</sup> Applications for these polymers include electronic devices such as organic photovoltaics (OPVs),<sup>2,3</sup> organic light-emitting diodes (OLEDs),<sup>4,5</sup> organic field-effect transistors (OFETs),<sup>6,7</sup> photorefractive devices,<sup>8</sup> and environmental sensors.<sup>9–13</sup> Among these materials, poly(phenylene ethynylenes) (PPEs), a class of conjugated polymers featuring a pattern of alternating aromatic rings and triple bonds, have stood out for their stability, moderate fluorescence quantum yields,<sup>14,15</sup> and readily tunable band gap.<sup>16,17</sup> The macromolecular assembly of PPEs in solution and thin films can be tuned from densely packed linear organizations to well-defined helical coiled or zigzag structures<sup>18</sup> by varying the substitution pattern (*para*, *meta*, *ortho*) of the aromatic rings along the backbone of the polymer chain. The classical syntheses of PPEs rely on step-growth polymerizations based on either transition-metal-catalyzed cross-coupling reactions or alkyne cross-metathesis (ACM).<sup>19,20</sup> While ACM and cyclodepolymerization of linear polymers have previously been used to access cyclic topologies, the thermodynamic products of these reactions are usually small cyclic oligomers comprised of not more than 3–6

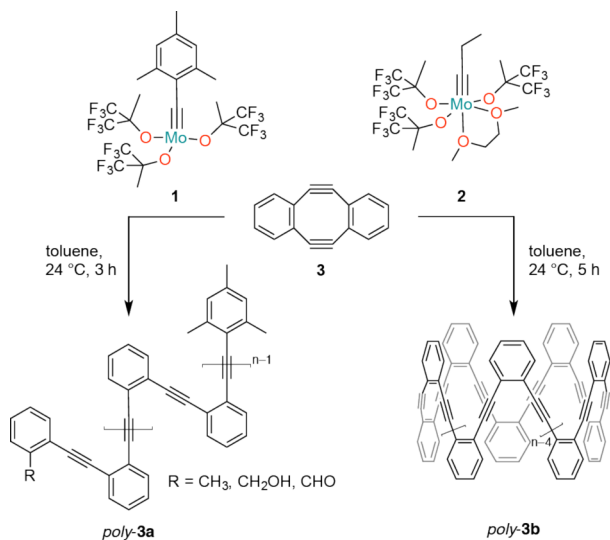
alkynes.<sup>21–24</sup> Transition-metal catalyzed cross-coupling polymerizations of aryl halides with aromatic alkynes, instead, suffer from undesired termination reactions, e.g., dehalogenation, and structural defects along the polymer backbone such as butadiyne groups emerging from oxidative coupling of terminal alkynes. While these strategies benefit from readily accessible monomers, they lack the precise control over degree of polymerization ( $X_n$ ), molecular weight, end-group functionality, and polydispersity index (PDI) unique to a controlled ring-opening alkyne metathesis polymerization (ROAMP) mechanism.<sup>25–27</sup>

In this study we report a novel route toward fully conjugated PPEs based on two ROAMP catalysts,  $[\text{MesC}\equiv\text{Mo}(\text{OC}(\text{CH}_3)(\text{CF}_3)_2)_3]$  (**1**) and  $[\text{EtC}\equiv\text{Mo}(\text{OC}(\text{CH}_3)(\text{CF}_3)_2)_3(\text{DME})]$  (**2**; DME = 1,2-dimethoxyethane) (Scheme 1) that selectively yield PPEs featuring either linear or cyclic polymer topology. Both catalysts rapidly initiate the polymerization of ring-strained monomer 5,6,11,12-tetrahydrobenzo[*a,e*][8]annulene (**3**) to form poly(*o*-phenylene ethynylene) (PoPE) featuring a mesityl or an ethyl end-group, respectively. Time-resolved NMR spectroscopy reveals that the active chain ends of the polymers featuring a mesityl end-group are stable under the reaction conditions. In

Received: March 6, 2016

Published: April 27, 2016

**Scheme 1. Synthesis of Linear Poly-3a and Cyclic Poly-3b from Ring-Strained Monomer 3 Using ROAMP Catalysts 1 and 2**



the absence of monomer, living polymers formed from **2** instead undergo highly regioselective backbiting into the least sterically hindered alkyne (EtC≡C) at the end-group to give cyclic PoPE with  $n > 5$  and the starting catalyst **2**. We herein demonstrate an unprecedented structural control over polymer topology by taking advantage of the unique selectivities of two ROAMP catalysts to form either linear or cyclic fully conjugated polymers derived from ring-strained monomers.

## RESULTS AND DISCUSSION

Catalyst **1** was synthesized from Mo(CO)<sub>6</sub> and MesLi following a procedure described by Tamm.<sup>28</sup> The DME adduct of catalyst **2** was obtained through cross-metathesis of the nitrido-complex [N≡Mo(OC(CH<sub>3</sub>)(CF<sub>3</sub>)<sub>2</sub>)<sub>3</sub>] with hex-3-yne as described by Johnson.<sup>29</sup> Orange prisms of **2** suitable for X-ray crystallography were obtained from a saturated toluene solution at -35 °C. The geometry at the Mo center is pseudo-octahedral. X-ray crystallography of **2** (Figure 1) confirms the presence of a C(1)≡Mo(1) triple bond with a bond length of 1.736(2) Å and a C(2)–C(1)–Mo(1) angle of 176.44(19)°. Three hexafluoro-*tert*-butoxide ligands adopt a meridional conformation featuring typical Mo(1)–O(1), Mo(1)–O(2), and Mo(1)–O(3) distances of 1.9632(15), 1.9326(15), and 1.9720(15) Å, respectively. In the crystal structure, 1 equiv of DME is coordinated to the Mo complex. The bond distances are 2.2283(15) and 2.4526(15) Å for the Mo(1)–O(4) *cis* and Mo(1)–O(5) *trans* to the carbyne, respectively. In solution, the octahedral complex **2** is in dynamic equilibrium with the pentacoordinate monodentate DME complex and the fully DME-dissociated tetracoordinate complex.<sup>30</sup> At 24 °C in benzene, the equilibrium lies on the side of the associated complexes **2** ( $K_d = 6.2 \times 10^{-5}$  mol L<sup>-1</sup>) (Supporting Information, Figure S1). Variable-temperature NMR reveals that the exchange is fast, suggesting that an open coordination site is readily available to bind the alkyne substrate.

We studied the ROAMP of 5,6,11,12-tetrahydrobenzo-*[a,e]*[8]annulene (**3**) with **1** and **2** (Scheme 1).<sup>31</sup> Addition of **1** to a solution of **3** (50 mM) in toluene ([**3**]/[**1**] = 10) at 24 °C leads to the precipitation of polymers within 1 h. <sup>1</sup>H and <sup>19</sup>F NMR indicate that **1** quantitatively initiates with a half-life of

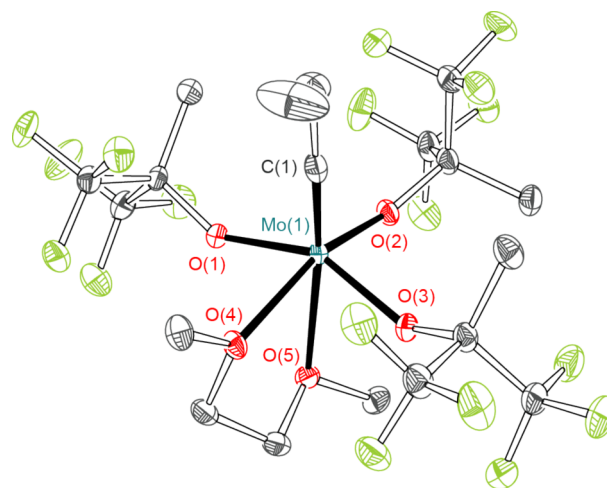


**Figure 1.** ORTEP representation of the X-ray crystal structure of **2**. Thermal ellipsoids are drawn at the 50% probability level. Color coding: C (gray), O (red), F (green), Mo (turquoise). Hydrogen atoms are omitted for clarity.

$t_{1/2} \ll 1$  min to form the propagating species. Monomer **3** is consumed in less than 1 h at 24 °C. The active ROAMP catalyst remains attached to the growing polymer chain. The molecular weight of the resulting polymers scales linearly with monomer conversion (Supporting Information, Figure S2).

Precipitation of the resulting polymer with MeOH affords poly-**3a** in 82% isolated yield. Gel permeation chromatography (GPC) analysis for various [**3**]/[**1**] loadings at 24 °C in toluene shows a PDI of 1.3–1.7 (Table 1). The molecular weights of

**Table 1.** Molecular Weight Analysis of Poly-**3a**

| [ <b>3</b> ]/[ <b>1</b> ] | $M_n$  |                  | $M_w$            |         | PDI |
|---------------------------|--------|------------------|------------------|---------|-----|
|                           | theory | GPC <sup>b</sup> | GPC <sup>b</sup> | $X_n^c$ |     |
| 10/1                      | 2134   | 1700             | 3000             | 11      | 1.7 |
| 20/1                      | 4134   | 4800             | 6400             | 21      | 1.3 |
| 30/1 <sup>a</sup>         | 6134   | 6600             | 9400             | 29      | 1.4 |

<sup>a</sup>[**3**]/[**1**] loadings >30 lead to precipitation of insoluble polymers before all monomer is consumed. <sup>b</sup>Calibrated to narrow polydispersity polystyrene standards. <sup>c</sup>Degree of polymerization determined by <sup>1</sup>H NMR end-group analysis.

poly-**3a** determined by GPC, calibrated to polystyrene standards, scale with the conversion of monomer, are proportional to the initial [**3**]/[**1**] loading, and show a unimodal distribution (Figure 2A). Extended reaction times do not lead to a broadening of the PDI. Mass spectrometry of polymers that have been quenched with MeOH is consistent with the characteristic signature for one mesityl end-group and a statistical mixture of CH<sub>3</sub>, CH<sub>2</sub>OH, or CHO end-groups resulting from the cleavage of the propagating molybdenum carbyne species (Supporting Information, Figure S3). While the <sup>1</sup>H NMR of poly-**3a** features two distinct resonance signals in the aromatic region, the <sup>13</sup>C NMR reveals a characteristic upfield shift for the alkyne carbon resonances (109.5 ppm in **3** to 92.6 ppm in poly-**3a**) associated with the release of the ring-strain stored in **3**. No evidence for branching or the formation of cyclic polymers could be observed by <sup>1</sup>H NMR analysis and mass spectrometry. End-group analysis of the mesityl group resonance signals (<sup>1</sup>H NMR) indicates that GPC overestimates the  $M_n$  of poly-**3a**. A correction factor of 1.1–1.2 correlates well

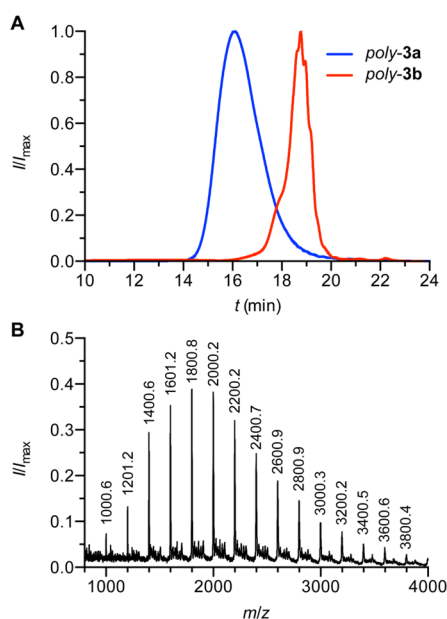


**Figure 2.** (A) GPC traces for linear poly-3a and purified cyclic poly-3b obtained through ROAMP of **3** with catalyst **1** and **2**, respectively, calibrated to polystyrene standards. (B) MALDI mass spectrum of cyclic poly-3b showing integer multiples of the mass of monomer **3** ( $MW = 200 \text{ g mol}^{-1}$ ) and the absence of end-groups.

with the degree of polymerization ( $X_n$ ) determined by NMR analysis and the expected molecular weight based on the initial  $[3]/[1]$  loading.

If the polymerization of **3** is initiated with the molybdenum propylidyne complex **2** ( $[3]/[2] = 10$ ) at  $24^\circ\text{C}$  in toluene no precipitation of polymers can be observed. Catalyst **2**

quantitatively reacts with **3** to form a propagating molybdenum complex ( $t_{1/2} \ll 1 \text{ min}$ ) as indicated by  $^1\text{H}$  and  $^{19}\text{F}$  NMR. Addition of MeOH to the homogeneous reaction mixture leads to the precipitation of poly-3b. GPC analysis of samples prepared from various  $[3]/[2]$  loadings at  $24^\circ\text{C}$  in toluene indicates the formation of discrete cyclic oligomers (poly-3b) and some higher molecular weight linear polymers ( $M_n = 5000\text{--}10000$ ) resulting from intermolecular cross-metathesis of living polymer chains. The ratio of products emerging from an intra- vs intermolecular chain transfer is concentration dependent, ranging from 93% cyclic polymers at  $[2] = 1 \text{ mM}$  to 86% at  $[2] = 10 \text{ mM}$  as determined by  $^1\text{H}$  NMR (Supporting Information, Table S1, Figures S4 and S5). The linear polymers can be removed by Soxhlet extraction or fractional precipitation to give pure cyclic poly-3b in >60% isolated yield (Figure 2A). Mass spectrometry of poly-3b shows evenly spaced peaks corresponding to integer multiples of **3** ( $m/z = [n \times 200] \text{ g mol}^{-1}$ ,  $n = 5, 6, 7, \dots, 20$ ; Figure 2B). The absence of end-groups in poly-3b is further corroborated by  $^1\text{H}$  and  $^{13}\text{C}$  NMR spectroscopy (Supporting Information, Figures S15 and S16) and highlights the unusual selectivity of catalyst **2** for the formation cyclic poly-3b over linear poly-3a.

To gain insight into the reaction mechanism, we studied the ROAMP of  $^{13}\text{C}$ -labeled **3\*** with **1**. In the presence of monomer, the resting state of the catalyst observed by  $^{13}\text{C}$  NMR is the interconverting metallacyclobutadienes **1a** and **1b** (Figure 3A, and Supporting Information, Figures S6 and S8), characterized by two broad sets of  $^1\text{H}$  and  $^{19}\text{F}$  resonances for the alkoxides (axial and equatorial) and two sets of  $^{13}\text{C}$  resonances for the metallacyclobutadiene carbons (one  $\beta$  carbon and two  $\alpha$  carbons).<sup>30,32</sup> Following the consumption of **3\***, the metallacyclobutadiene **1b** undergoes a final cycloreversion to give the labeled, ring-opened molybdenum benzylidyne complex **1c**. In

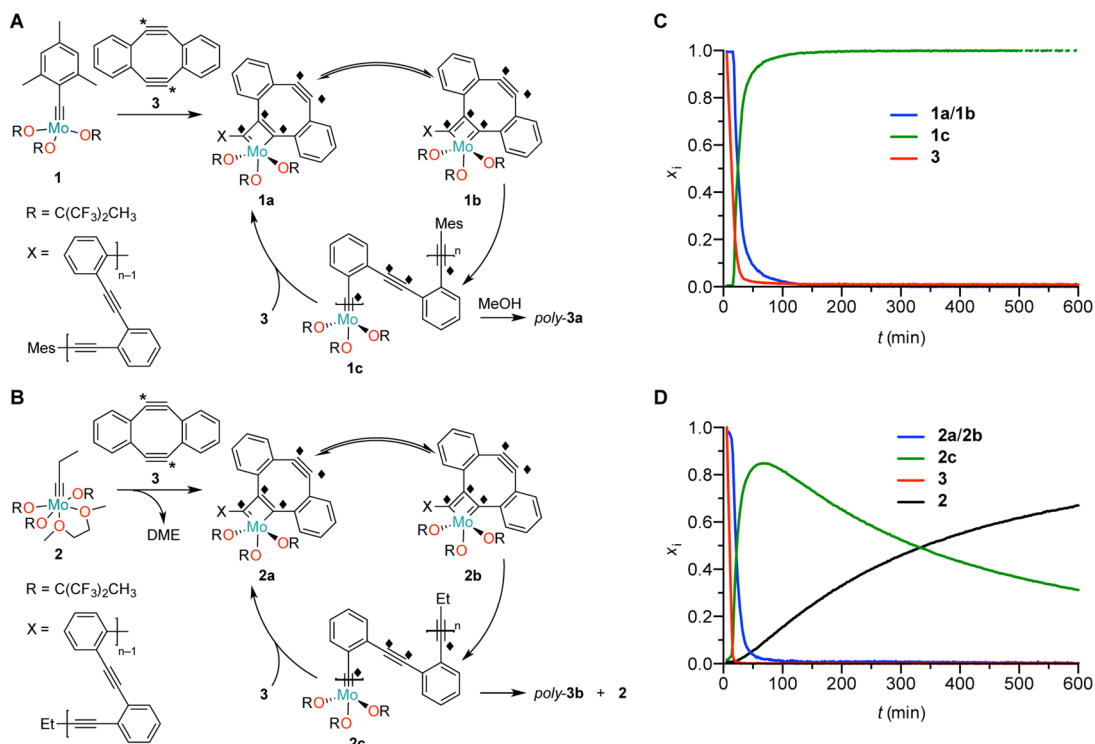


**Figure 3.** ROAMP of isotopically labeled **3\*** with catalyst **1** (A) and **2** (B) followed by time-resolved  $^1\text{H}$ ,  $^{19}\text{F}$ , and  $^{13}\text{C}$  NMR spectroscopy. Mole fraction of transient intermediates during the reaction of **1** (C) and **2** (D) with **3** derived from  $^1\text{H}$  NMR. Isotopic labeling: \*, 99.5%  $^{13}\text{C}$ ; ♦, 50%  $^{13}\text{C}$ .

the absence of monomer, **1c** is stable for >10 h and remains attached to one end of the polymer chain pending MeOH solvolysis. If the same polymerization is performed with **2**, the dominant molybdenum species observed in  $^{13}\text{C}$  NMR are the interconverting metallacyclobutadienes **2a** and **2b** (Figure 3B, and Supporting Information, Figures S7 and S9). Following the consumption of monomer, **2b** undergoes a final cycloreversion to give the ring-opened molybdenum benzylidyne complex **2c**. While **1c** is stable in the reaction mixture, **2c** undergoes highly regioselective backbiting into the butynyl end-group to give cyclic poly-**3b** and the original unlabeled molybdenum propylidyne complex **2**. The outstanding selectivity of this backbiting reaction is reflected in the absence of half-integer multiples of the monomer ( $m/z = [n \times 200 + 100]$  g mol $^{-1}$ ) in the mass spectrum of poly-**3b** (Figure 2B). The increased steric demand of internal alkynes lining the backbone of the growing polymer chain (**2c**) prevents a stochastic backbiting process and directs the reaction exclusively toward the unhindered butynyl end-group. Kinetic studies using [TolC≡Mo(OC(CH $_3$ )(CF $_3$ ) $_2$ ) $_3$ (DME)] (**4**) as a model complex for the propagating species **2c** show that the rate of cross-metathesis with the sterically less demanding 1-(but-1-yn-1-yl)-2-methylbenzene (**5a**) is  $\sim 200$  times faster ( $k = 1.3 \times 10^{-1} \text{ M}^{-1} \text{ s}^{-1}$ ) than with 1,2-bis(*o*-tolyl)acetylene (**5b**,  $k = 7.1 \times 10^{-4} \text{ M}^{-1} \text{ s}^{-1}$ ) (Supporting Information, Figures S10 and S11). The subtle kinetic selectivity that directs the intramolecular cross-metathesis of **2c** toward the sterically less hindered butynyl end-group has previously been observed for acyclic diyne metathesis (ADMET).<sup>21</sup>

The topological difference between linear and cyclic polymers, poly-**3a** and poly-**3b**, is reflected in their photo-physical properties. Although the UV–vis absorption spectra of poly-**3a** and poly-**3b** appear similar (Figure 4), cyclic poly-**3b**

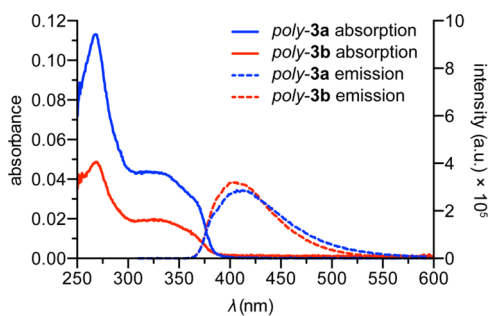


**Figure 4.** UV–vis absorption and fluorescence emission ( $\lambda_{\text{ex}} = 300$  nm) of linear poly-**3a** and cyclic poly-**3b** in chloroform solution (1.6 and 0.6  $\mu\text{g}/\text{mL}$  poly-**3a** and poly-**3b**, respectively).

exhibits a higher fluorescence quantum yield upon excitation at 300 nm ( $\Phi_{\text{F}} = 8.4\%$  and 18.6% for poly-**3a** and poly-**3b**, respectively). As the emission spectrum does not shift to longer wavelengths, the observed enhancement can not be explained by the formation of excimer complexes between adjacent monomer units as has been observed for e.g. cyclic polystyrene.<sup>33</sup> Instead, enhanced quantum yield can be attributed to the reduced conformational entropy of cyclic poly-**3b**. Cyclic poly-**3b** experiences less nonradiative relaxation than linear poly-**3a** due to the restricted intramolecular rotation about the polymer backbone.<sup>34,35</sup> The unique control over polymer topology enables tuning the mechanical and photo-physical properties of P $\rho$ PEs with minimal effect on their electronic structure.

## CONCLUSION

We describe the synthesis of a fully conjugated poly(*o*-phenylene ethynylene) using living ring-opening alkyne metathesis polymerization. Tuning the steric demand of the molybdenum carbyne initiator directs the synthesis of either linear or cyclic polymers with high selectivity. The polymerization mechanism and catalyst resting states were investigated through multinuclear NMR kinetic and  $^{13}\text{C}$  labeling studies. The catalyst system described herein represents an extraordinary access to the field of conjugated organic materials, simultaneously enabling exceptional control over polymer structure, sequence and topology.

## EXPERIMENTAL SECTION

**Materials and General Methods.** Unless otherwise stated, all manipulations of air and/or moisture sensitive compounds were carried out in oven-dried glassware, under an atmosphere of Ar or N $_2$ . All solvents and reagents were purchased from Alfa Aesar, Spectrum Chemicals, Acros Organics, TCI America, and Sigma-Aldrich and were used as received unless otherwise noted. Organic solvents were dried by passing through a column of alumina and were degassed by vigorous bubbling of N $_2$  or Ar through the solvent for 20 min. Flash column chromatography was performed on SiliCycle silica gel (particle size 40–63  $\mu\text{m}$ ). Thin layer chromatography was carried out using SiliCycle silica gel 60 Å F-254 precoated plates (0.25 mm thick) and visualized by UV absorption. All  $^1\text{H}$ ,  $\{^1\text{H}\}^{13}\text{C}$ , and  $^{19}\text{F}$  NMR spectra were recorded on Bruker AV-600, DRX-500, and AV-500 spectrometers, and are referenced to residual solvent peaks (CDCl $_3$ ,  $^1\text{H}$  NMR  $\delta = 7.26$  ppm,  $^{13}\text{C}$  NMR  $\delta = 77.16$  ppm; C $_6$ D $_6$ ,  $^1\text{H}$  NMR  $\delta = 7.16$  ppm,  $^{13}\text{C}$  NMR  $\delta = 128.06$  ppm; Tol- $d_8$ ,  $^1\text{H}$  NMR  $\delta = 2.08$  ppm; THF- $d_8$ ,  $^1\text{H}$  NMR  $\delta = 1.78$  ppm,  $^{13}\text{C}$  NMR  $\delta = 67.21$  ppm) or hexafluorobenzene ( $^{19}\text{F}$  NMR  $\delta = -162.90$  ppm). The concentrations of **4**, **5a**, and **5b** were determined by  $^1\text{H}$  and  $^{19}\text{F}$  NMR using the ERETIC method<sup>36</sup> against an external standard of 18.2 mM 1,3,5-tris(trifluoromethyl)benzene in C $_6$ D $_6$ . ESI mass spectrometry was performed on a Finnigan LTQFT spectrometer (Thermo) in positive ionization mode. MALDI mass spectrometry was performed on a Voyager-DE PRO spectrometer (Applied Biosystems Voyager System 6322) in positive mode using a matrix of dithranol. Elemental analysis (CHN) was performed on a PerkinElmer 2400 Series II combustion analyzer (values are given in %). GPC was carried out on an Agilent 1260 Infinity LC/MS setup with a guard and two Agilent Polypore 300  $\times$  7.5 mm columns at 35  $^\circ\text{C}$ . All GPC analyses were performed on a 0.2 mg/mL solution of polymer in chloroform. An injection volume of 25  $\mu\text{L}$  and a flow rate of 1 mL/min were used. Calibration was based on narrow polydispersity polystyrene standards ranging from  $M_{\text{w}} = 100$  to 4,068,981. X-ray crystallography was performed on APEX II QUAZAR, using a Microfocus Sealed Source (Incoatec I $\mu\text{S}$ ; Mo  $K\alpha$  radiation), Kappa Geometry with DX (Bruker-AXS build) goniostat, a Bruker APEX II detector, QUAZAR multilayer mirrors as the radiation monochromator, and Oxford Cryostream 700 for **2**. Crystallographic data was refined with SHELXL-97, solved with SIR-2007, visualized with ORTEP-32, and finalized with WinGX. UV–vis absorption spectra were acquired in chloroform solution on a Varian Cary 50 spectrophotometer (Agilent, USA). Fluorescence emissions spectra were acquired at an excitation wavelength of 300 nm on a Fluoromax-4 spectrofluorometer equipped with automatic polarizers, 1.0 nm slit widths for excitation/emission, and a 0.5 s integration time. Quantum yields were calibrated to 1,4-bis(5-phenyloxazol-2-yl)benzene (POPOP) in cyclohexane ( $\Phi_{\text{F}} = 0.97$ ).<sup>37</sup> **1**,<sup>28</sup> **3**,<sup>38</sup> **4**,<sup>31</sup> and **5b**<sup>39</sup> were synthesized following literature procedures.

**Preparation of [EtC≡Mo(OC(CH $_3$ )(CF $_3$ ) $_2$ ) $_3$ (DME)] (**2**).** A 100 mL sealable Schlenk flask was charged under N $_2$  with N≡Mo(OC(CF $_3$ ) $_2$ CH $_3$ ) $_3$  (1.00 g, 1.53 mmol) and 3-hexyne (1.25 g, 15.2 mmol) in toluene (50 mL) and heated to 95  $^\circ\text{C}$  for 20 h. The reaction mixture was cooled to 24  $^\circ\text{C}$ , 1,2-dimethoxyethane (156 mg, 1.73 mmol) was added, and stirred for 30 min. The solvent was removed under vacuum. The residue was extracted with Et $_2$ O (20

mL), filtered through Celite, concentrated to 5 mL under vacuum and cooled to  $-35\text{ }^{\circ}\text{C}$ . The precipitate was collected by filtration. Recrystallization from pentane ( $-35\text{ }^{\circ}\text{C}$ ) yielded **2** (0.69 g, 0.90 mmol, 58%). Crystals for X-ray analysis were grown from toluene.  $^1\text{H}$  NMR (600 MHz,  $\text{C}_6\text{D}_6$ ,  $22\text{ }^{\circ}\text{C}$ )  $\delta$  = 3.16 (s, 6H,  $(\text{CH}_3\text{OCH}_2)_2$ ), 3.00 (s, 4H,  $(\text{CH}_3\text{OCH}_2)_2$ ), 2.65 (q,  $J$  = 7.6 Hz, 2H,  $\text{MoCCH}_2\text{CH}_3$ ), 1.71 (s, 9H,  $\text{OC}(\text{CF}_3)_2\text{CH}_3$ ), 0.59 (t,  $J$  = 7.6 Hz, 3H,  $\text{MoCCH}_2\text{CH}_3$ ) ppm;  $^{13}\text{C}$  NMR (151 MHz,  $\text{C}_6\text{D}_6$ ,  $22\text{ }^{\circ}\text{C}$ )  $\delta$  = 309.8 (MoCEt), 124.5 (q,  $^1J_{\text{CF}}$  = 289 Hz,  $\text{OC}(\text{CF}_3)_2\text{CH}_3$ ), 83.3 (m,  $^2J_{\text{CF}}$  = 29 Hz,  $\text{OC}(\text{CF}_3)_2\text{CH}_3$ ), 71.6 ( $(\text{CH}_3\text{OCH}_2)_2$ ), 63.8 ( $(\text{CH}_3\text{OCH}_2)_2$ ), 43.1 ( $\text{MoCCH}_2\text{CH}_3$ ), 18.9 ( $\text{OC}(\text{CF}_3)_2\text{CH}_3$ ), 12.6 ( $\text{MoCCH}_2\text{CH}_3$ ) ppm;  $^{19}\text{F}$  NMR (376 MHz,  $\text{C}_6\text{D}_6$ ,  $22\text{ }^{\circ}\text{C}$ )  $\delta$  =  $-78.84$  ppm; FTMS (ESI-TOF)  $m/z$  for  $[\text{EtC}\equiv\text{Mo}(\text{OC}(\text{CH}_3)(\text{CF}_3)_2)_3]^+$  calcd  $[\text{C}_{15}\text{H}_{14}\text{F}_{18}\text{MoO}_3]$ , 681.9710; found, 681.9720; Anal. Calcd for  $[\text{EtC}\equiv\text{Mo}(\text{OC}(\text{CH}_3)(\text{CF}_3)_2)_3(\text{DME})]$ : C, 29.62; H, 3.14. Found: C, 29.35; H, 2.96. Crystal data: CCDC no. 1456633; formula,  $\text{C}_{19}\text{H}_{24}\text{F}_{18}\text{MoO}_3$ ; fw, 770.32  $\text{g mol}^{-1}$ ; temp, 100(2) K; cryst. system, monoclinic; space group,  $P2(1)/n$ ; color, black;  $a$ , 11.4678(9) Å;  $b$ , 16.8911(14) Å;  $c$ , 13.8634(11) Å;  $\alpha$ ,  $90.000^{\circ}$ ;  $\beta$ ,  $91.155(2)^{\circ}$ ;  $\gamma$ ,  $90.000^{\circ}$ ;  $V$ , 2684.8(4) Å<sup>3</sup>;  $Z$ , 4;  $R_1$ , 0.0262;  $wR_2$ , 0.0556; GOF, 1.197.

**Preparation of Linear Poly(o-phenylene ethynylene) (Poly-3a).** A 5 mL vial was charged under  $\text{N}_2$  with **3** (0.02 g, 0.10 mmol) in toluene (1.50 mL). **1** (3.8 mg, 5.0  $\mu\text{mol}$ ) in toluene (0.60 mL) was added at  $24\text{ }^{\circ}\text{C}$  and the mixture was stirred for 3 h. The reaction mixture was quenched with MeOH (10 mL). The solid precipitate was isolated by filtration and washed with MeOH (30 mL) to yield poly-**3a** (0.02 g, 82%) as a brown solid.  $^1\text{H}$  NMR (500 MHz,  $\text{CDCl}_3$ ,  $22\text{ }^{\circ}\text{C}$ )  $\delta$  = 7.56–7.45 (br, 56H), 7.20–7.09 (br, 56H), 6.81 (s, 2H), 2.46 (s, 6H), 2.24 (s, 3H) ppm;  $^{13}\text{C}$  NMR (126 MHz,  $\text{CDCl}_3$ ,  $22\text{ }^{\circ}\text{C}$ )  $\delta$  = 132.3, 128.1, 125.8, 92.6, 21.3 ppm.

**Preparation of Cyclic Poly(o-phenylene ethynylene) (Poly-3b).** A 20 mL vial was charged under  $\text{N}_2$  with **3** (0.06 g, 0.30 mmol) in toluene (1.50 mL). **2** (43.4 mg, 55.0  $\mu\text{mol}$ ) in toluene (0.50 mL) was added at  $24\text{ }^{\circ}\text{C}$  and the mixture was stirred for 24 h. The reaction mixture was quenched with MeOH (10 mL). The solid precipitate was isolated by filtration and washed with MeOH (30 mL). Soxhlet extraction (hexane) of the crude mixture yielded poly-**3b** (0.01 g, 18%) as a brown solid. The polymer remaining in the extraction thimble (30 mg) was dissolved in chloroform (15 mL) and precipitated with pentane (60 mL). After the precipitate was filtered off, the filtrate was evaporated to yield additional pure poly-**3b** (0.02 g, total yield 50%).  $^1\text{H}$  NMR (600 MHz,  $\text{CDCl}_3$ ,  $22\text{ }^{\circ}\text{C}$ )  $\delta$  = 7.48–7.44 (m, 2H), 7.13–7.09 (m, 2H) ppm;  $^{13}\text{C}$  NMR (126 MHz,  $\text{CDCl}_3$ ,  $22\text{ }^{\circ}\text{C}$ )  $\delta$  = 132.2, 128.1, 125.7, 92.5 ppm.

## ■ ASSOCIATED CONTENT

### ● Supporting Information

The Supporting Information is available free of charge on the ACS Publications website at DOI: 10.1021/jacs.6b02422.

Figures S1–S11; Table S1; methods and instrumentation; synthetic procedures for **7**, **8**, **3\***, and **5a**; characterization; kinetic experiments; DME dissociation studies; NMR spectra (Figures S12–S20); and X-ray crystallographic data (Table S2–S6) (PDF)

X-ray crystallographic information for **2** (CIF)

## ■ AUTHOR INFORMATION

### Corresponding Author

\*ffischer@berkeley.edu

### Author Contributions

‡S.K. and D.B. contributed equally.

### Notes

The authors declare no competing financial interest.

## ■ ACKNOWLEDGMENTS

This research is supported by the National Science Foundation under contract number CHE-1455289, Berkeley NMR Facility is supported in part by NIH Grant SRR023679A, and the X-Ray Facility is supported in part by NIH Shared Instrumentation Grant S10-RR027172. D.B. acknowledges fellowship support through the Abramson Foundation. The authors acknowledge Dr. Christian Canlas and Dr. Hasan Celik for support with NMR acquisition and Dr. Antonio DiPasquale for assistance with X-ray analysis.

## ■ REFERENCES

- (1) Scherf, U.; List, E. J. *Adv. Mater.* **2002**, *14* (7), 477–487.
- (2) Cheng, Y.-J.; Yang, S.-H.; Hsu, C.-S. *Chem. Rev.* **2009**, *109* (11), 5868–5923.
- (3) Weber, J.; Thomas, A. *J. Am. Chem. Soc.* **2008**, *130* (20), 6334–6335.
- (4) Friend, R. H.; Gymer, R. W.; Holmes, A. B.; Burroughes, J. H.; Marks, R. N.; Taliani, C.; Bradley, D. D. C.; Santos, D. A. D.; Brédas, J. L.; Lögdlund, M.; Salaneck, W. R. *Nature* **1999**, *397* (6715), 121–128.
- (5) Reineke, S.; Lindner, F.; Schwartz, G.; Seidler, N.; Walzer, K.; Lüssem, B.; Leo, K. *Nature* **2009**, *459* (7244), 234–238.
- (6) Kanimozhi, C.; Yaacobi-Gross, N.; Chou, K. W.; Amassian, A.; Anthopoulos, T. D.; Patil, S. *J. Am. Chem. Soc.* **2012**, *134* (40), 16532–16535.
- (7) Knopfmacher, O.; Hammock, M. L.; Appleton, A. L.; Schwartz, G.; Mei, J.; Lei, T.; Pei, J.; Bao, Z. *Nat. Commun.* **2014**, *5*, 2954.
- (8) Fuller, M. J.; Walsh, C. J.; Zhao, Y.; Wasielewski, M. R. *Chem. Mater.* **2002**, *14* (3), 952–953.
- (9) Yang, J.-S.; Swager, T. M. *J. Am. Chem. Soc.* **1998**, *120* (46), 11864–11873.
- (10) Smith, R. C.; Tennyson, A. G.; Lim, M. H.; Lippard, S. J. *Org. Lett.* **2005**, *7* (16), 3573–3575.
- (11) Wosnick, J. H.; Mello, C. M.; Swager, T. M. *J. Am. Chem. Soc.* **2005**, *127* (10), 3400–3405.
- (12) Hussain, S.; De, S.; Iyer, P. K. *ACS Appl. Mater. Interfaces* **2013**, *5* (6), 2234–2240.
- (13) Ryu, S.; Yoo, I.; Song, S.; Yoon, B.; Kim, J.-M. *J. Am. Chem. Soc.* **2009**, *131* (11), 3800–3801.
- (14) Intemann, J. J.; Hellerich, E. S.; Tlach, B. C.; Ewan, M. D.; Barnes, C. A.; Bhuwalka, A.; Cai, M.; Shinar, J.; Shinar, R.; Jeffries-EL, M. *Macromolecules* **2012**, *45* (17), 6888–6897.
- (15) Jagtap, S. P.; Mukhopadhyay, S.; Coropceanu, V.; Brizius, G. L.; Brédas, J.-L.; Collard, D. M. *J. Am. Chem. Soc.* **2012**, *134* (16), 7176–7185.
- (16) Zhao, X.; Pinto, M. R.; Hardison, L. M.; Mwaura, J.; Müller, J.; Jiang, H.; Witker, D.; Kleiman, V. D.; Reynolds, J. R.; Schanze, K. S. *Macromolecules* **2006**, *39* (19), 6355–6366.
- (17) Guo, X.; Watson, M. D. *Macromolecules* **2011**, *44* (17), 6711–6716.
- (18) Kübel, C.; Mio, M. J.; Moore, J. S.; Martin, D. C. *J. Am. Chem. Soc.* **2002**, *124* (29), 8605–8610.
- (19) Bunz, U. H. F. *Macromol. Rapid Commun.* **2009**, *30* (9–10), 772–805.
- (20) Yang, H.; Jin, Y.; Du, Y.; Zhang, W. *J. Mater. Chem. A* **2014**, *2* (17), 5986–5993.
- (21) Zhang, W.; Moore, J. S. *J. Am. Chem. Soc.* **2005**, *127* (33), 11863–11870.
- (22) Zhang, W.; Brombosz, S. M.; Mendoza, J. L.; Moore, J. S. *J. Org. Chem.* **2005**, *70* (24), 10198–10201.
- (23) Gross, D. E.; Moore, J. S. *Macromolecules* **2011**, *44* (10), 3685–3687.
- (24) Yang, H.; Liu, Z.; Zhang, W. *Adv. Synth. Catal.* **2013**, *355* (5), 885–890.
- (25) Zhang, W.; Moore, J. S. *Adv. Synth. Catal.* **2007**, *349* (1–2), 93–120.

- (26) Jyothish, K.; Zhang, W. *Angew. Chem., Int. Ed.* **2011**, *50* (37), 8478–8480.
- (27) Fürstner, A. *Angew. Chem., Int. Ed.* **2013**, *52* (10), 2794–2819.
- (28) Haberlag, B.; Freytag, M.; Daniliuc, C. G.; Jones, P. G.; Tamm, M. *Angew. Chem., Int. Ed.* **2012**, *51* (52), 13019–13022.
- (29) Gdula, R. L.; Johnson, M. J. A. *J. Am. Chem. Soc.* **2006**, *128* (30), 9614–9615.
- (30) Freudenberger, J. H.; Schrock, R. R.; Churchill, M. R.; Rheingold, A. L.; Ziller, J. W. *Organometallics* **1984**, *3* (10), 1563–1573.
- (31) Bellone, D. E.; Bours, J.; Menke, E. H.; Fischer, F. R. *J. Am. Chem. Soc.* **2015**, *137* (2), 850–856. Strained 5,6,11,12-tetrahydrobenzo[*a,e*][8]annulene (**3**) decomposes rapidly at  $T > 40$  °C and was thus incompatible with the ROAMP catalyst reported in ref 31.
- (32) O'Reilly, M. E.; Ghiviriga, I.; Abboud, K. A.; Veige, A. S. *Dalton Trans.* **2013**, *42* (10), 3326–3336.
- (33) Gan, Y.; Dong, D.; Carlotti, S.; Hogen-Esch, T. E. *J. Am. Chem. Soc.* **2000**, *122* (9), 2130–2131.
- (34) Hong, Y.; Lam, J. W. Y.; Tang, B. Z. *Chem. Commun.* **2009**, *29*, 4332–4353.
- (35) Zhu, X.; Zhou, N.; Zhang, Z.; Sun, B.; Yang, Y.; Zhu, J.; Zhu, X. *Angew. Chem., Int. Ed.* **2011**, *50* (29), 6615–6618.
- (36) Akoka, S.; Barantin, L.; Trierweiler, M. *Anal. Chem.* **1999**, *71* (13), 2554–2557.
- (37) Lakowicz, J. R. *Principles of Fluorescence Spectroscopy*, 2nd ed.; Kluwer Academic Publishers: Amsterdam, 1999.
- (38) Orita, A.; Hasegawa, D.; Nakano, T.; Otera, J. *Chem. - Eur. J.* **2002**, *8* (9), 2000–2004.
- (39) Chuentragool, P.; Vongnam, K.; Rashatasakhon, P.; Sukwattanasinitt, M.; Wacharasindhu, S. *Tetrahedron* **2011**, *67* (42), 8177–8182.